ACS OMEGA

http://pubs.acs.org/journal/acsodf

Article

Upgrading Wood Gas Using Bentonite Clay: A Multiscale Modeling and Simulation Study

Matthew Lasich*

Cite This: https://dx.doi.org/10.1021/acsomega.0c00937

Read Online

ACCESS | Metrics & More | Article Recommendations

ABSTRACT: Wood gas is the producer gas resulting from gasification of wood biomass and is an important renewable fuel gas in rural areas. This study assessed the capacity of bentonite, a widely used clay mineral, to upgrade wood gas via pressure swing adsorption in order to improve its calorific value (i.e., the amount of energy released per kilogram of gas). Grand canonical Monte Carlo molecular simulations using a self-consistent force field were performed to generate adsorption isotherms for wood gas components—methane, carbon monoxide, carbon dioxide, hydrogen, nitrogen, and oxygen—in montmorillonite (the main crystalline constituent of bentonite) at conditions appropriate to downdraft gasification. The Langmuir adsorption isotherm model was successfully fitted to each component's adsorption isotherm and was then coupled with a batch equilibrium approach to model a single-stage pressure swing adsorption system with a discharge stream at ambient pressure. A response surface was then computed in terms of the net change in the calorific value as a function of both adsorbent quantity and operating pressure. It was found that the system can improve the calorific value of the gas by over five percent.

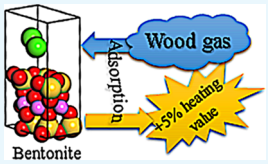

1. INTRODUCTION

Biomass gasification is the conversion of carbonaceous materials into a gaseous producer gas consisting of nitrogen, carbon monoxide, carbon dioxide, methane, hydrogen, and water, which may be used as a feedstock for conversion into higher-value chemicals or for fuel. When wood or related materials are used as the carbonaceous feedstock, the resulting producer gas is typically referred to as "wood gas". Utilizing biomass energy, such as by gasification, is important to enhance the sustainability of the energy supply system, especially in rural areas.[1] There have not been many implementations of biomass gasification systems in South Africa since the 1960s[2] despite biomass being identified as a key potential renewable energy source in the country.[3]

Previous work developed a pressure swing adsorption scheme in order to upgrade landfill gas to pipeline-grade methane.[4] Biogas upgrading by adsorption using activated carbon[5] and metal−organic frameworks[6] has also been examined previously, along with using low-pressure vacuum swing adsorption.[7] Upgrading natural gas using cryogenic pressure−temperature swing adsorption has been studied in the literature, specifically using zeolite 13X.[8] MILENA gasification technology[9] should also be mentioned in which synthetic natural gas is derived from biomass gasification and subsequently upgraded using an alternative route to those mentioned earlier: absorption. Apart from adsorption processes, zeolites and clays have been examined as catalysts for conversion of carbon monoxide/hydrogen blends[10] and for upgrading biofuels.[11]

This study examines the use of bentonite clay to upgrade wood gas by enhancing its calorific value through the process of pressure swing adsorption. The conditions of interest for this study were those pertaining to downdraft gasification (i.e., T = 973 K), which is suitable for use with internal combustion engines,[12] such as may be found in electric generators in rural areas. Pure species adsorption isotherms were generated for methane, carbon monoxide, carbon dioxide, hydrogen, nitrogen, and oxygen in montmorillonite (the primary constituent of bentonite). These isotherms were then coupled with a batch equilibrium modeling approach to assess pressure swing adsorption over a range of adsorbent bed sizes and operating pressure ratios in order to improve the calorific value of the wood gas. Higher-value wood gas would result in more energy being available for use in rural and peri-urban areas and may help to stimulate economic activities in such areas in the developing world.

2. RESULTS AND DISCUSSION

2.1. Adsorption Isotherms. Pure species absolute adsorption isotherms at 973 K are shown in Figure 1. It is apparent that complications related to the wood gas composition may affect attempts at improving the calorific value by considering the relative uptake of the gas species from highest to lowest: $H_2 > O_2 > CO > N_2 > CH_4 > CO_2$. This series illustrates that the non-calorific species O_2 and N_2 adsorb to a

Received: March 2, 2020
Accepted: April 29, 2020

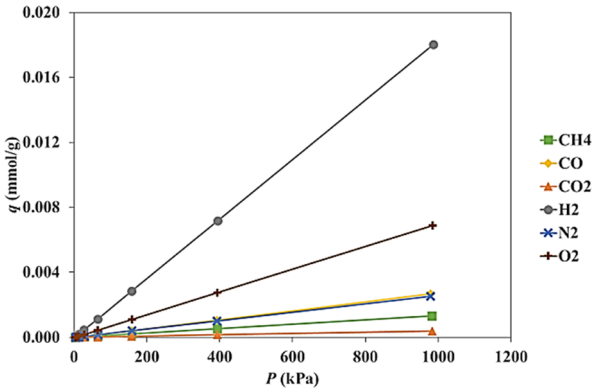

Figure 1. Adsorption isotherms at 973 K for all of the species of interest in this study. The quantity of gas adsorbed into the solid is q, and P is the pressure. Lines between the points are guides for the eye. Error bars are smaller than the symbols.

large degree compared to the calorific species CO and CH_4, and thus, caution should be taken when the composition of raw wood gas is inconsistent, as it would invariably produce inconsistencies in the degree to which the calorific value is enhanced. It can be noted that the adsorption isotherms shown are apparently linear; this is largely due to relatively low pressures considered in this study. The limitations on the range of pressures to be studied are tied to the aims of the study in terms of assisting in the development of a low-cost adsorption system that is easy to fabricate in rural and peri-urban areas.

Fitting the Langmuir adsorption equation to the data presented in Figure 1 was successful in all cases, with correlation coefficients (R^2) being no less than 0.9996 for all species. The fitted Langmuir parameters (i.e., q_0 and K), RMSE values, and correlation coefficients are presented in Table 1. While the maximum uptake capacity of hydrogen is the largest among all of the species forming wood gas, the pressure dependencies of carbon dioxide, oxygen, and nitrogen are larger. This suggests that non-monotonic behavior may be expected when examining the calorific value of upgraded wood gas when using montmorillonite as an adsorbent, which will be demonstrated in the following sections.

Table 1. Fitted Langmuir Adsorption Mode Parameters q_0 and K along with the Root-Mean-Square Error (RMSE) and the Correlation Coefficient (R^2)

species	q_0 (mmol/g)	K (kPa^{-1})	RMSE	R^2
CH_4	1.821×10^{-2}	7.776×10^{-5}	1.034×10^{-5}	0.9999
CO	3.336×10^{-2}	8.684×10^{-5}	2.515×10^{-5}	0.9998
CO_2	4.082×10^{-3}	1.049×10^{-4}	4.268×10^{-6}	0.9996
H_2	1.964×10^{-1}	1.001×10^{-4}	1.696×10^{-4}	0.9997
N_2	2.685×10^{-2}	1.038×10^{-4}	2.726×10^{-5}	0.9997
O_2	7.331×10^{-2}	1.035×10^{-4}	6.722×10^{-5}	0.9997

2.2. Calorific Value. Performance of the bentonite pressure swing adsorption system was considered over the ranges $1.5 \leq P^* \leq 8.5$ and 5×10^3 g/mol $\leq W \leq 50 \times 10^3$ g/mol. Since the aim was to examine systems that can potentially be fabricated using only basic tools, it was determined that the operating pressure (i.e., P_{ad}) should not be too high, thereby limiting the uppermost adsorption pressure under consideration. Examination of the pure species adsorption isotherms suggested that an adsorber bed size in the region of 10^3 g per mole of feed gas may be appropriate, hence the range for W considered in this study.

The relationship between the higher and lower heating values and the adsorber bed size (W) and operating pressure ratio (P^*) are shown in Figures 2 and 3, respectively. In both cases, optimal performance is obtained at low operating pressures and large adsorber bed sizes although there is larger variation in terms of the HHV as compared to the LHV. In terms of the magnitude of upgrading that was obtained, a maximum enhancement of 5.38% was achieved for the HHV at $P^* = 1.5$ and $W = 50 \times 10^3$ g/mol, while for the LHV, an improvement of 4.84% was obtained at the same conditions as for the HHV.

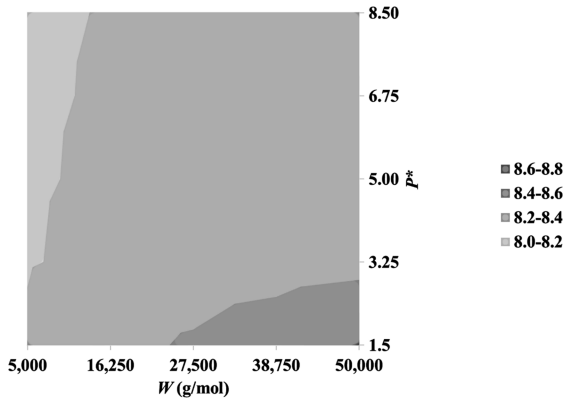

Figure 2. Response surface for the higher heating value (HHV) of wood gas (in MJ/kg) in terms of adsorbent quantity (W) and operating pressure ratio ($P^* = P_{ad}/P_{de}$).

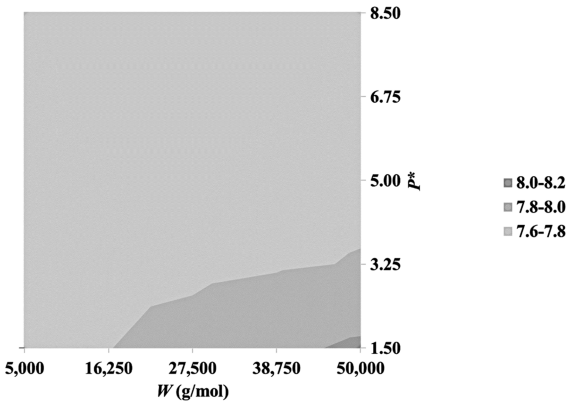

Figure 3. Response surface for the lower heating value (LHV) of wood gas (in MJ/kg) in terms of adsorbent quantity (W) and operating pressure ratio ($P^* = P_{ad}/P_{de}$).

The slight differences in trends for the HHV and LHV are largely due to differences in separation of the combustible species in wood gas; carbon monoxide combustion does not involve water, while hydrogen and methane combustion does. Therefore, variation in the methane and hydrogen content may of course affect the relationship between the LHV and the HHV for wood gas. The relative difference in the heating value in terms of HHV compared to LHV is about 18% for hydrogen and 11% for methane. Therefore, adsorbing hydrogen in particular from the feed gas is likely to cause significant differences between the HHV and LHV, which was observed in Figures 2 and 3 since Figure 1 demonstrated that montmorillonite does adsorb hydrogen preferentially compared to any other species comprising wood gas.

https://dx.doi.org/10.1021/acsomega.0c00937
ACS Omega XXXX, XXX, XXX−XXX

2.3. Stoichiometric Oxygen Requirements. The stoichiometric oxygen requirement is a feature that combines a measure of the composition of the combustible gases within the product gas with the amount of residual air and is shown in Figure 4. Based on the stoichiometry of the combustion

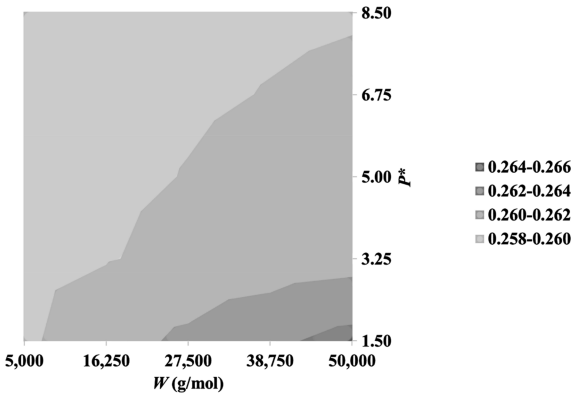

Figure 4. Response surface for the stoichiometric oxygen requirement (O_2^{req}) of wood gas (in moles of O_2 per mole of gas) in terms of adsorbent quantity (W) and operating pressure ratio ($P^* = P_{ad}/P_{de}$).

reactions, 2:1 for carbon monoxide and hydrogen and 1:2 for methane, in terms of the moles of gas species per mole of oxygen, it is apparent that methane-rich wood gas will likely have a higher stoichiometric oxygen requirement. However, this can be muted somewhat if large quantities of residual air from the gasification process remain (since air is composed of nitrogen and oxygen). The pure species adsorption isotherms (see Figure 1) demonstrated that montmorillonite preferentially adsorbs oxygen compared to nitrogen although the selectivity toward methane adsorption lies in between hydrogen and carbon monoxide.

Compared to the baseline of 0.259 mole of O_2 per mole of gas (computed using the feed gas composition), it is apparent that treatment with pressure swing adsorption using bentonite as the adsorbent is likely to increase the stoichiometric oxygen requirement, largely by enhancing the composition of combustible gases within the wood gas. The maximum value for O_2^{req} was obtained for $W = 50 \times 10^3$ g/mol and $P^* = 1.50$ and amounted to an increase of approximately 2.20% compared to the feed gas. Taken in conjunction with the effect of pressure swing adsorption on the calorific value, this suggests that the heating value of wood gas can be increased disproportionately to the increases in the oxygen requirement. This observation can be useful in the context of using upgraded wood gas in internal combustion engines for performing work or generating electricity.

2.4. Overall Gas Recovery. In addition to considering improvements and changes in the wood gas' performance as a potential fuel, the efficiency of the proposed pressure swing adsorption system should also be considered in terms of the proportion of the gas that gets discarded in the process. This was considered by computing the overall quantity of gas that is discharged as the product gas as a proportion of the raw gas before treatment. In this case, it is apparent that the operating conditions necessary for the largest improvements in the heating value of the gas also correspond with the region at which most of the gas does not make it into the product stream in the first pass through the pressure swing adsorption system, as shown in Figure 5. This suggests that the performance of any practical

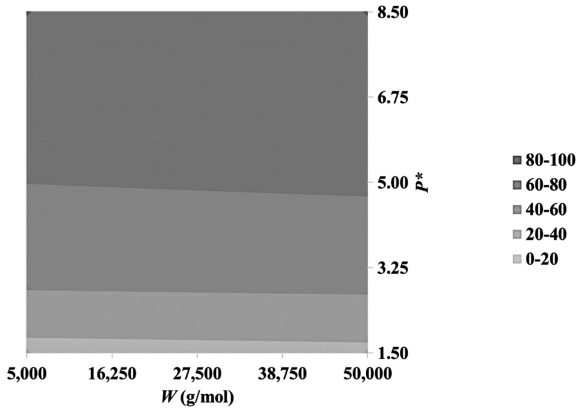

Figure 5. Response surface for the percentage of overall gas recovery of wood gas (in terms of the number of moles recovered versus the number of moles entering the system) in terms of adsorbent quantity (W) and operating pressure ratio ($P^* = P_{ad}/P_{de}$).

system can depend on the performance criteria used to assess the design since an improved calorific value will come at the cost of either increased wood gas wastage or in having a large gas recycle system.

2.5. Carbon Dioxide Removal. In view of carbon taxes playing increasingly prominent roles in industrial operations worldwide, it was also necessary to examine the potential carbon dioxide removal in this study. Unfortunately, the removal of carbon dioxide followed a similar general trend to the gas recovery but in reverse. In other words, having a lower overall gas recovery resulted in more carbon dioxide removal, as shown in Figure 6. This unfavorable observation may be related to the

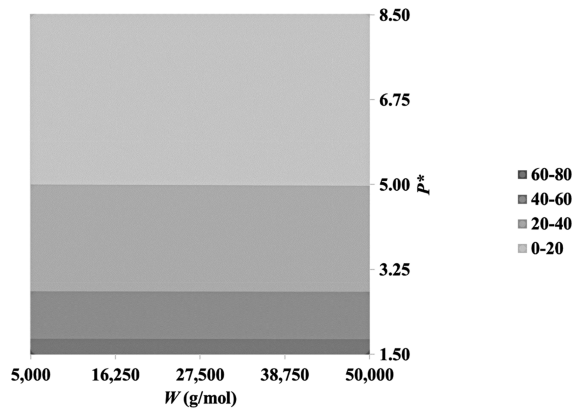

Figure 6. Response surface for the percentage of carbon dioxide in the feedstock that was removed, shown in terms of adsorbent quantity (W) and operating pressure ratio ($P^* = P_{ad}/P_{de}$).

selectivities of the gas species at lower pressures shown in Figure 1, where it was shown that all of the species besides hydrogen and oxygen are broadly similar in terms of uptake into montmorillonite. However, this particular trend may not be practically important for small-scale wood gasification operations (which is likely applicable in many rural and peri-urban settings), as in many countries, there are lower thresholds below which carbon taxation does not apply. While carbon emissions may of course be problematic from combustion using raw or upgraded wood gas, an inherent advantage is that provided the feedstock for gasification is sourced responsibly, the net carbon

https://dx.doi.org/10.1021/acsomega.0c00937
ACS Omega XXXX, XXX, XXX−XXX

emissions over the entire life cycle of the operation may not be too problematic.

3. CONCLUSIONS

Multiscale modeling was undertaken to examine the utility (or otherwise) of pressure swing adsorption to upgrade wood gas through the use of bentonite as an adsorbent. Monte Carlo molecular simulations in the grand canonical ensemble were used to generate adsorption isotherms, which were subsequently coupled with a batch equilibrium modeling approach to model a pressure swing adsorption system over a range of operating pressures and adsorbent bed sizes.

The performance of the adsorption system was described using several features: the heating value of the output gas (in terms of HHV and LHV), stoichiometric oxygen requirement, overall gas recovery, and fractional removal of carbon dioxide. It was found that an improvement in the HHV of over 5% could be obtained although at the cost of reduced gas recovery. Increases in the heating value were found to be disproportionate compared to the increases in the stoichiometric oxygen requirement due to subtle changes in the composition of the wood gas as it passed through the adsorption system.

It is recommended that other adsorbents be examined that can also serve as adsorbents for the purposes of upgrading or enhancing renewable producer gases, especially those that can be produced in rural and peri-urban areas. In particular, focus should be given to adsorbents that are readily attainable in developing and undeveloped countries and regions in order to have the largest potential impact in terms of increasing energy availability in these areas.

4. METHODOLOGY

4.1. Bentonite Structure. Bentonite is a clay mineral available locally in South Africa (there is a commercially exploited deposit near Heidelberg in the Western Cape province) that consists chiefly of crystalline montmorillonite.[13] Therefore, compacted montmorillonite was used as a proxy for bentonite in this study, similar to recent work on the use of bentonite as an adsorbent for humid air.[14] Bentonite has wide use in the food and beverage industry as a purification medium, as drilling mud, as a foundry binder, and as a protein adsorbent, among other uses.[15] Bentonite has also been studied in the last decade for applications as diverse as separating oil from water,[16] the development of clay/rubber nanocomposites,[17] and in radioactive waste disposal.[18]

A crystalline calcium-rich montmorillonite structure from the literature[18] was used in this study, which had an orthogonal unit cell 0.518 nm × 0.898 nm × 1.500 nm in size with the chemical formula $O_{24}Al_4Si_8Ca_2$. The crystal unit cell is presented in Figure 7, demonstrating disorder in the crystal in the form of random shifts, which produced the best fit to experimental data.[19] However, the structure is not fully disordered since the different layers of the crystal do not possess different translations and rotations with respect to a common axis.

4.2. Simulation Details. Monte Carlo simulations employing the Metropolis scheme[20] were used to simulate adsorption of the wood gas components carbon monoxide, carbon dioxide, methane, hydrogen, nitrogen, and oxygen into the montmorillonite lattice. The reader is referred to previous work[21] using Monte Carlo simulation for a detailed discussion on the adsorption of methane in fractal nanopores, in which the gas-in-place, excess adsorption, and absolute adsorption isotherms are

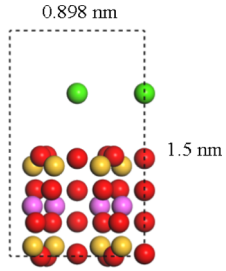

Figure 7. Ball model of the montmorillonite unit cell. The color coding of the atoms is as follows: white = hydrogen, red = oxygen, orange = silicon, green = calcium, and pink = aluminum (color available online).

described for such systems. The Metropolis algorithm is a stochastic process that generates a set of sample configurations from the selected ensemble, which can be used to determine average thermophysical properties. In the case of gas adsorption into pores within a solid, the relevant ensemble was the grand canonical ensemble in which the temperature, solid volume, and gas-phase chemical potential were held constant. The Metropolis scheme entails transforming a system of molecules via a two-step process: first, a trial configuration is generated by application of a randomly applied action on the system and second, that move is either rejected or accepted on the basis of the change in the energy of the system of particles. In the event that the trial configuration is accepted, the configuration of the system is transformed, and in this way, a Markov chain of configurations is generated of which a subset is sampled to generate results of equilibrium properties.

The probability ρ of a configuration m in the grand canonical ensemble is given by[22]

$$\rho_m = CF(\{N\}_m)\exp[-\beta E_m] \tag{1}$$

in which C is a normalization constant, $\{N\}_m$ is the set of all loadings of the gas molecules within the solid lattice associated with configuration m, β is the reciprocal of the absolute temperature, and E is the total energy of the configuration computed using the relevant force field. $F(N)$ is a function for a single component, which is given by

$$F(N) = [(\beta f V)^N / N!]\exp[-\beta N \mu_{\text{intra}}] \tag{2}$$

wherein f is the fugacity of the gas species, and μ_{intra} is its intramolecular chemical potential averaged over the ensemble. The probability P of accepting a transition from state m to n is then computed using

$$P_{m\to n} = \min[1, \rho_n/\rho_m] \tag{3}$$

Thus, transitions to more likely (typically lower energy) configurations are accepted while less probable transitions are unlikely to be accepted. The Peng−Robinson cubic equation of state[23] was used to convert between pressure and chemical potential for the molecular simulations. This equation of state is widely used in natural gas processing and related areas of chemical engineering and is one of the best two-constant cubic equations of state.[24]

In this study, the following Monte Carlo moves were applied to the gas particles (with probabilities of occurrence in parentheses): creation (23%), deletion (23%), rotation (24%), translation (24%), and regrowth (6%). The first two moves mimic adsorption and desorption, respectively, while the remaining moves mimic thermal motion of the adsorbed molecules within the crystal. The atoms constituting the solid

https://dx.doi.org/10.1021/acsomega.0c00937
ACS Omega XXXX, XXX, XXX−XXX

were held fixed since it is not a fluid material and serves as a rigid framework for the purposes of this work. To equilibrate the system, 10^6 Monte Carlo moves were used, with further 10^7 moves being used to generate results. For each data point in this study, five independent simulations were performed to obtain the final results.

All intermolecular interactions in this study were described using version 2.8 of the fully atomistic condensed-phase optimized molecular potentials for atomistic simulation studies (COMPASS) force field.[25] The COMPASS force field accounts for bonds, bond angles, dihedral angles, out-of-plane angles, van der Waals interactions, and electrostatic interactions. A cutoff radius of 1.85 nm with an analytical tail correction was used for the van der Waals interactions, and the highly accurate Ewald summation technique was employed for the electrostatic interactions.[26] The van der Waals interactions are described using the 9-6 Lennard-Jones potential[27] coupled with the Waldman−Hagler[28] combining rules in the COMPASS force field. The simulation cell consisted of six montmorillonite unit cells (constructed by arranging 3 × 2 × 1 unit cells together), similar to previous work[14] that showed this to be the minimum system size necessary to avoid periodicity errors[29] when simulating adsorption in montmorillonite. Alternatives to the COMPASS force field that are also fully atomistic include the PCFF[30] and DREIDING[31] force fields. Both COMPASS and PCFF are described as consistent force fields although PCFF is older, and recent work[32] employing COMPASS showed good agreement with experimental data[33] in terms of hydrogen sulfide adsorption relative to nitrogen in another silicate material (cement hydrate). Moreover, the COMPASS force field has already been used to successfully model adsorption of humid air in montmorillonite.[14] Therefore, COMPASS was deemed appropriate for this study.

All simulations were performed over the fugacity range of 0.1−1000 kPa at T = 973 K. As mentioned in section 1 above, this temperature is typically the exit temperature from downdraft gasification, which is typically the appropriate gasification process to employ for internal combustion engines.[12] As the intention of this work was to introduce as few elements as possible into downstream wood gas upgrading, the exit temperature of the gasifier was used so as to not have to employ cooling in between gasification and adsorption. As stated earlier, the fugacity and chemical potential for each species were related to its pressure by use of the Peng−Robinson cubic equation of state. The 2018 version of the Materials Studio computer program[34] was used for the Monte Carlo simulations shown in this study.

4.3. Adsorption Isotherms. Following the procedure outlined above, adsorption isotherms were generated for all the species of interest. However, the adsorption isotherm results were not used directly, and adsorption isotherm modeling was undertaken so that the fitted models could be used in subsequent process modeling calculations. As demonstrated in section 2.1, adsorption for all systems was accurately described using the simplistic Langmuir model.[35] This description of adsorption is predicated on several assumptions: adsorption site equivalence, immobility of adsorbed molecules, single-site occupancy, surface homogeneity, and no interactions between adsorbate molecules. Mathematically, this relationship has the form

$$q = q_0 KP/(1 + KP) \tag{4}$$

wherein q is the quantity of gas adsorbed, q_0 represents the maximum uptake of gas in the adsorbent, K is the fitted Langmuir constant, and P is the pressure of the gas reservoir. This expression can be represented in terms of either pressure or fugacity, but the results shown in this study are in pressure terms for ease of understanding. Fitting the Langmuir equation to the results of the molecular simulations was undertaken using the root-mean-square error (RMSE) as the objective function for minimization

$$\mathrm{RMSE} = [\Sigma(q_{\mathrm{fit}} - q_{\mathrm{sim}})^2/p]^{0.5} \tag{5}$$

in which q_{fit} is the fitted uptake of gas, q_{sim} is the result from the molecular simulations, and p is the total number of data points per isotherm. It can be noted that eq 4 can be linearized in various ways, thereby yielding simple linear expressions that when used to plot experimental or simulated results, can rapidly indicate whether the Langmuir model is appropriate. Due to the relatively low pressures of the systems being investigated, it was expected that single-site Langmuir adsorption would occur; however, at higher pressures, it can be expected that a dual-site Langmuir model may be necessary, as discussed in the literature.[21]

4.4. Batch Equilibrium Modeling. Pressure swing adsorption at 973 K was undertaken for a typical wood gas consisting of 50.9 vol % nitrogen, 27.0 vol % carbon monoxide, 14.0 vol % hydrogen, 4.5 vol % carbon dioxide, 3.0 vol % methane, and the remainder oxygen.[36] Modeling the adsorption system was undertaken using a batch equilibrium approach,[37] which described the system as a cycle with an unchanging amount of solid adsorbent. Material balances for the adsorption and desorption stages yield the adsorbed quantities of each species in the solid and gas phases, and solving these balances yields the final product composition. Of the gases constituting wood gas, it would be desirable to remove non-calorific gases such as nitrogen, carbon dioxide, and oxygen in order to improve the calorific value in terms of MJ/kg. Retaining oxygen in the product gas may, however, be helpful in terms of lowering the stoichiometric oxygen requirements for situations in which insufficient excess oxygen may be available, albeit at the cost of a reduced calorific value.

Figure 8 illustrates the batch equilibrium approach. In order to determine the final composition of the product gas, the

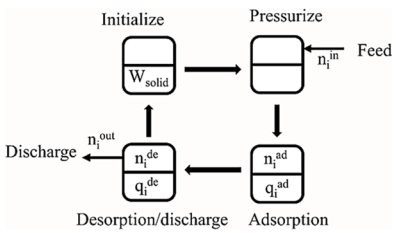

Figure 8. Diagram illustrating the batch equilibrium approach.

following material balances must be solved simultaneously for every species i

$$n_i^{\mathrm{in}} = n_i^{\mathrm{ad}} + q_i^{\mathrm{ad}} \tag{6}$$

$$n_i^{\mathrm{ad}} + q_i^{\mathrm{ad}} = n_i^{\mathrm{de}} + q_i^{\mathrm{de}} + n_i^{\mathrm{out}} \tag{7}$$

in which n and q refer to the amount of gas species i in the gaseous and solid phases, respectively, and the superscripts in, ad, de, and out refer to the feed, adsorption stage, desorption

https://dx.doi.org/10.1021/acsomega.0c00937
ACS Omega XXXX, XXX, XXX−XXX

stage, and discharge streams, respectively. In Figure 8, W_{solid} refers to the mass of solid adsorbent in each adsorber bed (note that there are two beds, which alternate in operation between the adsorption and desorption stages). The final product gas comprises the gaseous phase at the desorption stage. Equations 6 and 7were solved using a successive substitution approach, with a tolerance of 10^{-6} using $|\Delta n_{N2}{}^{de}|$ as the check for convergence. The batch equilibrium modeling calculations were undertaken using a routine written for GNU Octave version 5.1.0.[38] Analyses of the responses in the adsorption system were considered in terms of both W and the ratio of adsorption pressure to desorption pressure P^* (in which $P^* = P_{ad}/P_{de}$). In all cases, operation at atmospheric pressure was considered, i.e., P_{de} = 101.3 kPa.

In order to assess the efficacy of the pressure swing adsorption system, three features of the product gas were considered: the higher heating value (HHV), lower heating value (LHV), and the stoichiometric oxygen requirement ($O_2{}^{req}$). The HHV is the total heat of combustion of the product gas considered by returning all of the combustion components to 298 K, including condensation (particularly of water in this case). The LHV is the HHV minus the heat of vaporization of water, and so, differences in trends between the two heating values can readily indicate the extent to which the product gas is likely to form steam during combustion. As a baseline, the higher and lower heating values of the wood gas used as a feedstock in this study were calculated[39] as 8.1687 and 7.6609 MJ/kg, respectively. The stoichiometric oxygen requirement can be affected by the degree to which oxygen is removed from the wood gas; if a larger amount of oxygen is removed, then the stoichiometric oxygen requirement may increase although it should also be noted that oxygen itself is not adding a calorific value to the gas. The stoichiometric oxygen requirements were determined by considering complete combustion of carbon monoxide, methane, and hydrogen, yielding a baseline of 0.259 mole of O_2 per mole of feed gas.

■ AUTHOR INFORMATION

Corresponding Author

Matthew Lasich − *Department of Chemical Engineering, Mangosuthu University of Technology, Durban 4031, South Africa;* orcid.org/0000-0002-7849-6603; Email: lasich.matthew@mut.ac.za

Complete contact information is available at: https://pubs.acs.org/10.1021/acsomega.0c00937

Notes

The author declares no competing financial interest.

■ ACKNOWLEDGMENTS

All simulations were performed using the facilities of the Centre for High Performance Computing (CHPC) in Cape Town, South Africa. This work is supported by the National Research Foundation (NRF) through its Rated Researcher program.

■ REFERENCES

(1) Aoyagi, S.; Noda, R.; Horio, M.; Fujimara, H. Planning of Japanese forest biomass by existing power plants. In *Proceedings of the 68th Annual Meeting of the Society of Chemical Engineers of Japan*, Tokyo, Japan, 2003; p 115.

(2) Mamphweli, N. S.; Meyer, E. L. Implementation of the biomass gasification project for community empowerment at Melani village, Eastern Cape, South Africa. *Renewable Energy* **2009**, *34*, 2923−2927.

(3) Petrie, B.; Macqueen, D. *South African biomass energy: little heeded but much needed*; IIED Briefing website: https://pubs.iied.org/17165IIED/ (accessed Jan 21, 2020).

(4) Cavenati, S.; Grande, C. A.; Rodrigues, A. R. Adsorption equilibrium of methane, carbon dioxide, and nitrogen on zeolite 13X at high pressures. *J. Chem. Eng. Data* **2004**, *49*, 1095−1101.

(5) Vivo-Vilches, J. F.; Pérez-Cadenas, A. F.; Maldonado-Hódar, F. J.; Carrasco-Marín, F.; Faria, R. P. V.; Ribeiro, A. M.; Ferreira, A. F. P.; Rodrigues, A. R. Biogas upgrading by selective adsorption onto CO_2 activated carbon from wood pellets. *J. Environ. Chem. Eng.* **2017**, *5*, 1386−1393.

(6) Chaemchuen, S.; Kabir, N. A.; Zhou, K.; Verpoort, F. Metal-organic frameworks for upgrading biogas via CO_2 adsorption to biogas green energy. *Chem. Soc. Rev.* **2013**, *42*, 9304−9332.

(7) Aarya, A.; Divekar, S.; Rawat, R.; Gupta, P.; Garg, M. O.; Dasgupta, S.; Nanoti, A.; Singh, R.; Xiao, P.; Webley, P. A. Upgrading biogas at low pressure by vacuum swing adsorption. *Ind. Eng. Chem. Res.* **2015**, *54*, 404−413.

(8) Moreira, M. A.; Ribeiro, A. M.; Ferreira, A. F. P.; Rodrigues, A. E. Cryogenic pressure temperature swing adsorption process for natural gas upgrade. *Sep. Purif. Technol.* **2017**, *173*, 339−356.

(9) van der Meijden, C. M. Development of the MILENA Gasification Technology for the Production of Bio-SNG. Ph.D. Thesis, Eindhoven University of Technology, December 2010.

(10) Barrault, J.; Gatineau, L.; Hassoun, N.; Bergaya, F. Selective syngas conversion over mixed aluminum-iron pillared laponite clay. *Energy Fuels* **1992**, *6*, 760−763.

(11) Perego, C.; Bosetti, A.; Ricci, M.; Millini, R. Zeolite materials for biomass conversion to biofuel. *Energy Fuels* **2017**, *31*, 7721−7733.

(12) Basu, P. *Biomass Gasification and Pyrolysis: Practical Design and Theory*; Elsevier: Amsterdam, 2010; pp 167−228.

(13) Clem, A. G.; Doehler, R. W. Industrial applications of bentonite. *Clays Clay Miner.* **1961**, *10*, 272−283.

(14) Lasich, M.; Narasigadu, C.; Moodley, S. Adsorption of humid air in compacted montmorillonite: A Monte Carlo simulation study. *Fluid Phase Equilib.* **2019**, *487*, 52−57.

(15) Hosterman, J. W.; Patterson, S. H. *Bentonite and Fuller's Earth Resources of the United States*; U.S. Geological Survey: Washington DC, 1992.

(16) Mansur, C. R. E.; Oliveira, R. S.; Akeda, V.; Queirós, Y. G. C.; Spinelli, L. S.; Lucas, E. F. Nanocomposites based on ionene−bentonite used to treat oily water. *J. Appl. Polym. Sci.* **2012**, *123*, 218−226.

(17) Mat, N. S. C.; Ismail, H.; Othman, N. Curing characteristics and tear properties of bentonite filled ethylene propylene diene (EPDM) rubber composites. *Procedia Chem.* **2016**, *19*, 394−400.

(18) Shirazi, S. M.; Kazama, H.; Salman, F. A.; Othman, F.; Akib, S. Permeability and swelling characteristics of bentonite. *Int. J. Phys. Sci.* **2010**, *5*, 1647−1659.

(19) Viani, A.; Gualtieri, A. F.; Artioli, G. The nature of disorder in montmorillonite by simulation of X-ray powder patterns. *Am. Mineral.* **2002**, *87*, 966−975.

(20) Metropolis, N.; Rosenbluth, A. W.; Rosenbluth, M. N.; Teller, A. H.; Teller, E. Equation of state calculations by fast computing machines. *J. Chem. Phys.* **1953**, *21*, 1087−1092.

(21) Lin, K.; Huang, X.; Zhao, Y.-P. Combining image recognition and simulation to reproduce the adsorption/desorption behaviors of shale gas. *Energy Fuels* **2020**, *34*, 258−269.

(22) Frenkel, D.; Smit, B. *Understanding Molecular Simulation: From Algorithms to Applications*; Academic Press: San Diego, 2002.

(23) Peng, D. Y.; Robinson, D. B. A new two-constant equation of state. *Ind. Eng. Chem. Fundam.* **1976**, *15*, 59−64.

(24) Lopez-Echeverry, J. S.; Reif-Acherman, S.; Araujo-Lopez, E. Peng-Robinson equation of state: 40 years through cubics. *Fluid Phase Equilib.* **2017**, *447*, 39−71.

(25) Sun, H. COMPASS: an ab initio force-field optimized for condensed-phase applications overview with details on alkane and benzene compounds. *J. Phys. Chem. B* **1998**, *102*, 7338−7364.

(26) Ewald, P. P. Die Berechnung optischer und elektrostatischer Gitterpotentiale. *Ann. Phys.* **1921**, *369*, 253−287.

(27) Warshel, A.; Lifson, S. Consistent force field calculations. II. Crystal structures, sublimation energies, molecular and lattice vibrations, molecular conformations, and enthalpies of alkanes. *J. Chem. Phys.* **1970**, *53*, 582−594.
(28) Waldman, M.; Hagler, A. T. New combining rules for rare gas van der Waals parameters. *J. Comput. Chem.* **1993**, *14*, 1077−1084.
(29) Allen, M. P.; Tildesley, D. J. *Computer Simulation of Liquids*; Clarendon Press: Oxford, 1987.
(30) Sun, H.; Mumby, S. J.; Maple, J. R.; Hagler, A. T. An ab initio CFF93 all-atom force field for polycarbonates. *J. Am. Chem. Soc.* **1994**, *116*, 2978−2987.
(31) Mayo, S. L.; Olafson, B. D.; Goddard, W. A. DREIDING: a generic force field for molecular simulations. *J. Phys. Chem.* **1990**, *94*, 8897−8909.
(32) Lasich, M. Sorption of natural gas in cement hydrate by Monte Carlo simulation. *Eur. Phys. J. B* **2018**, *91*, 299.
(33) Jaber, M. B.; Couvert, A.; Amrane, A.; Le Cloirec, P.; Dumont, E. Removal of hydrogen sulfide in air using cellular concrete waste: Biotic and abiotic filtrations. *Chem. Eng. J.* **2017**, *319*, 268−278.
(34) Systémes, D. *Materials Studio 2018*; BIOVIA: San Diego, CA. 2017.
(35) Langmuir, I. The constitution and fundamental properties of solids and liquids. Part I. Solids. *J. Am Chem. Soc.* **1916**, *38*, 2221−2295.
(36) Taylor, C. F. *Internal-Combustion Engine in Theory and Practice* MIT Press: Cambridge, 1985 *Vol. 1* pp 46−47.
(37) Chung, Y.; Na, B. K.; Song, H. K. Short-cut evaluation of pressure swing adsorption systems. *Comput. Chem. Eng.* **1998**, *22*, S637−S640.
(38) Eaton, J. W.; Bateman, D.; Hauberg, S. *GNU Octave Version 5.1.0 Manual: a High-Level Interactive Language for Numerical Computations*. https://www.gnu.org/software/octave/doc/v5.1.0/ (accessed Feb 28, 2020).
(39) Engineering ToolBox *Gross and Net Heating Values for Some Common Gases*; https://www.engineeringtoolbox.com/gross-net-heating-values-d_420.html (accessed Feb 29, 2020).

https://dx.doi.org/10.1021/acsomega.0c00937
ACS Omega XXXX, XXX, XXX−XXX